A comparative study of hydroxyethylcellulose-based solid polymer electrolytes for solid state Zn batteries

Received: 15 October 2022 | Revised: 22 November 2022 | Accepted: 28 November 2022

DOI: 10.1002/nano.202200221

RESEARCH ARTICLE

Nano Select Open Access WILEY

A comparative study of hydroxyethylcellulose-based solid polymer electrolytes for solid state Zn batteries

Amandine Brige[1] | **Martina Olsson**[2] | **Shizhao Xiong**[2,3] | **Aleksandar Matic**[2,3]

[1]Department of Chemistry, École Normale Supérieure, PSL University, Paris, France

[2]Department of Physics, Chalmers University of Technology, Göteborg, Sweden

[3]Wallenberg Wood Science Centre, Chalmers University of Technology, Gothenburg, Sweden

Correspondence
Aleksandar Matic, Department of Physics, Chalmers University of Technology, SE 412 96, Göteborg, Sweden.
Email: matic@chalmers.se

Abstract

Rechargeable zinc metal batteries are greener and safer alternative to lithium batteries, but they suffer from poor reversibility due to growth of zinc dendrites and water splitting reactions of aqueous electrolytes. One strategy to overcome these drawbacks is replacing aqueous electrolyte with solid polymer electrolyte (SPE). In this work, we examine the possibility of fabricating solid electrolyte from a bio-based polymer, hydroxyethylcellulose (HEC), with the aim to further increase the sustainability of zinc batteries. Various types of zinc salts, drying procedures and the salt concentrations are investigated for their impact on the ionic conductivity, structure, and phase behavior of as-prepared polymer electrolytes. It is found that HEC has a good film-forming ability compared with commonly used poly(ethylene oxide) but its low salt-dissociation capability leads to an ionic conductivity of 10^{-6} S cm^{-1} even at the elevated temperature of 110°C, hindering the possibility of solely utilizing HEC as matrix of solid electrolyte. Our results suggest that introducing a new polymer with higher salt-dissociation capability or lower glass transition temperature into the HEC matrix can be a reliable way to build solid polymer electrolytes with sufficient ionic conductivity and good mechanical property for future zinc batteries.

KEYWORDS

bio-based polymer, conductivity, solid polymer electrolyte, structural properties, zinc battery

1 | INTRODUCTION

Low-cost and environment-friendly electrochemical energy storage devices are essential for a successful transition towards sustainability since they can solve the issue of intermittency of renewable power sources.[1–2] Current rechargeable batteries, which mostly rely on lithium chemistry, are widely used because of their high energy density and excellent cyclability. However, safety issues and limited abundance of lithium promote a strong interest in developing batteries based on new chemistries.[3] In this regard, zinc (Zn) is a promising candidate to replace lithium as active ion in rechargeable batteries. Zinc presents an inherent potential with respect to sustainability, cost, and energy density.[4–5] Its natural reserves are abundant, it possesses high theoretical volumetric capacity, and has a relatively low electrochemical potential (−0.76 V vs. standard hydrogen electrode).[6] In addition to these features, the insensitivity of Zn-metal to ambient conditions (oxygen and humidity) bears great promise for its utilization as a metal anode. When it is coupled with an aqueous electrolyte and an appropriate

cathode material, a safe and non-toxic battery technology can be expected.[7]

However, realizing Zn-metal batteries (ZIBs) faces a number of challenges. The use of aqueous electrolytes brings about issues such as water splitting, evaporation, leakage, and dissolution of cathode material.[8] Moreover, irregular deposition of Zn on the metal anode during charging induces the formation and quick growth of dendrites which are the root of poor cyclability, low efficiency, and eventual internal short-circuits.[9] These obstacles can be overcome by replacing the liquid electrolyte with a solid polymer electrolyte (SPE).[10–11] This alternative has the potential to drastically improve the stability towards the Zn metal anode by efficiently suppressing the growth of dendrites. In addition, SPEs can have high electrochemical stability and avoid issues with leakage and evaporation. This, in turn, can improve both capacity and cyclability. Besides these improvements, the flexibility of SPEs is of great interest for wearable electronic applications.[12]

SPEs consist of a polymer matrix in which a salt is dissolved, that is, the polymer chain itself solvates the ions without the presence of a liquid component.[13–15] Metal cations, such as Zn^{2+} in ZIBs or Li^{+} in Li-metal batteries, move along the polymer chains by successive coordination and dissociation with specific sites on the polymer.[16–17] Local chain motion and bond rotation help to break and reform polymer-cation complexes, enabling ion hopping from site to site and thereby long-range motion.[5,6] So far, the ionic conductivity of SPEs based on this transport mechanism is usually several orders of magnitude lower than that of liquid electrolytes. This is insufficient to realize SPEs in practical applications in batteries.[14] To obtain a SPE with high ionic conductivity, the polymer matrix should therefore be flexible, have a low glass transition temperature (T_g), and be able to dissolve the Zn-salt. Therefore, the selection of polymer matrix and Zn-salt is critical to achieve fast ion transport, along with mechanical strength, chemical and electrochemical stability, and interfacial compatibility.

For the choice of polymer matrix in SPEs, intensive research has been conducted on systems based on poly(ethylene oxide) (PEO, $[-CH_2-CH_2-O-]_n$).[12–13] In PEO, the metal cations are solvated by ether oxygen atoms on the polymer chain, without being immobilized. However, ion transport mainly occurs in the amorphous phase through segmental motion.[18] While this enables ion hopping from site to site, PEO is still highly crystalline at ambient temperature, with a melting point around 65–70°C.[19] Thus, modification strategies like adding plasticizers or using copolymers are explored to improve ion transport in PEO-based SPEs by decreasing the crystallinity and increasing the local polymer chain dynamics. Recently, there has been a growing interest in making SPEs out of bio-sourced polymers, which are made from renewable and sustainable raw materials.[20] Biopolymer-based SPEs show a great promise to achieve low-cost and environment-friendly batteries since their physical and chemical properties can be tuned by grafting functional groups of interest on the polymer backbone.[21] The development of biopolymer-based SPEs has so far been hampered by the use of water as a solvent during materials preparation. Whereas this is highly beneficial for sustainable production, it is not compatible with the water-sensitive lithium technology. For Zn-batteries, however, the presence of water is not an issue and a bio-sourced SPE fits perfectly to the desire of a green battery.[8,22] In particular, cellulose and its derivatives are very attractive candidates due to their good film-forming ability and mechanical strength.[23]

For the selection of salt for SPEs, there is a general principle that salts with low lattice energy will contribute to higher conductivity, since ion pairs dissociated, solvation of ions by the polymer chain, and ion motion along the chains are all facilitated. In this perspective, Zn-salts with bulky anions can be good candidates for SPEs since the negative charge is delocalized, resulting in weaker ionic bonds.[24–25] Bulky anions can also act as plasticizers to the polymer matrix and increase segmental motion, which in turn contributes to an enhanced ionic conductivity. In the field of Li-ion batteries, bis(trifluoromethanesulfonyl)imide (TFSI–) and trifluoromethanesulfonate (OTf–) are commonly used weakly coordinating anions.[5,24] However, in pursuit of a low-cost and eco-friendly technology, cheaper and greener salts would be welcome.

In the field of ZIBs, rational selection of polymer matrix and Zn-salt is important for the design of high performance SPEs, but little attention has so far been paid to this topic. Here we systematically investigate how the selection of polymer and Zn-salt affects the ionic conductivity of SPEs for ZIBs. A biopolymer derivative, hydroxyethylcellulose (HEC), is chosen as the polymer matrix. HEC has side chains of ethylene oxide groups grafted on the cellulose backbone. Since the side chains are too short to align in a regular pattern, HEC is fully amorphous. The results obtained for SPEs based on HEC are benchmarked to traditional PEO-based SPEs and the dependency of ionic conductivity and crystallinity of polymers on preparation conditions are discussed. Additionally, the role of Zn-salt and salt concentration in SPEs is investigated.

2 | RESULTS AND DISCUSSION

2.1 | Structure of SPE films

In this work, several Zn-salts have been selected to compare the influence of the salt on the physical properties

of HEC- and PEO- based solid polymer electrolytes. First of all, zinc sulfate ($ZnSO_4$) has been chosen since it is the most common Zn-salt used in aqueous electrolytes for Zn-batteries. $Zn(TFSI)_2$ and $Zn(OTf)_2$ have also been considered since TFSI– and OTf– are good plasticizers and weakly coordinating anions, traditionally used in lithium-SPEs. Zinc acrylate and zinc acetate have been selected as cheaper alternatives for the traditional SPE salts, with a possible plasticizing effect while being soluble in water. The polymer/Zn-salt solid electrolyte films were prepared by solvent casting under identical conditions, as detailed in the experimental section. The salt concentration was set to a ratio of ether oxygens to Zn ions ($EO:Zn^{2+}$) of 20:1.[26–27] For safety and sustainability reasons, water was selected as solvent since it is capable of dissolving all chemicals, and is an environment-friendly solvent.

As shown in Figure 1A, the distribution of Zn-salt and rigidity of poly(ethylene oxide) (PEO) based films varies with the anion of the Zn-salt. Using Zn acetate, Zn sulfate and Zn acrylate results in rigid, self-standing films, while using $Zn(OTf)_2$ and $Zn(TFSI)_2$, which both act as plasticizers, results in highly flexible and sticky films. The $PEO/Zn(TFSI)_2$ film is very soft and hardly self-standing HEC, on the other hand, shows a better film-forming ability, even if the HEC-based films are more brittle and less flexible than the PEO ones. It can also be noticed from visual inspection of the films that the crystallinity of PEO films is highly dependent on the drying conditions. As shown in Figure 1B, crystals are macroscopical in the PEO-based film dried at ambient temperature, which is not observed for the sample dried at 50°C in Figure 1A. In contrast, all hydroxyethylcellulose (HEC)-based films are homogenous and transparent, without any visible defects.

Wide-angle X-ray scattering (WAXS) was used to probe the crystallinity of the samples. The broad peak in the WAXS profile of HEC shows the signature of the amorphous structure (Figure 2A). In contrast, crystalline Zn-salts show sharp, characteristic peaks in their WAXS curves, see Figure S1. For most HEC/Zn-salt films, only small peaks related to salt crystallinity appear in the WAXS curves, indicating that the Zn-salts are mostly, but not fully, dissolved in the HEC-matrix. It is consistent with the transparent and homogeneous appearance of the films observed by naked eye. The HEC/Zn sulfate film is less transparent and has apparent inhomogeneities, and its WAXS profile also presents the strongest crystalline peaks among the HEC films. It confirms that Zn sulfate does not dissolve well in HEC. The poor affinity between polymer and Zn sulfate has been explained by Zhang et al., who linked it to the strong salting-out ability of $ZnSO_4$ according to the Hofmeister series.[28–29] Despite its use in aqueous electrolytes for Zn-ion batteries, $ZnSO_4$ is therefore not suitable for HEC and PEO SPEs.

The numerous sharp peaks in the WAXS profile of the PEO film demonstrates the high degree of crystallinity of the polymer (Figure 2B). Characteristic peaks from the salt appear in all PEO/Zn-salt films curves, except for $PEO/Zn(TFSI)_2$, showing that the Zn-salts are not fully dissolved by the PEO matrix. The increased intensity of the broad amorphous halos in the background of the crystalline peaks for $PEO/Zn(TFSI)_2$ and $PEO/Zn(OTf)_2$ indicate a decrease in the crystallinity of the polymer matrix, confirming the plasticizing effect of TFSI– and OTf–. The plasticizing behavior of OTf– and TFSI– is also visible for HEC-based films through a slight shift of the peak to higher q and a broadening of the main peak. This broadening indicates an increased variety of interchain distances, which can be a consequence of the insertion of anions between the polymer chains.[30]

The chemical structure of the polymer electrolytes was further investigated by Fourier-transform infrared spectroscopy (FTIR) as shown in Figure 2C and D. For both PEO/Zn-salt and HEC/Zn-salt samples, new peaks corresponding to anions appear in addition to those of the polymers. The main bands originating from the polymer structure are not much affected by the presence of the salt. However, it can be noticed that the bands at 1059, 1044, and 1093 cm^{-1} in PEO and at 1050 cm^{-1} in HEC, which are attributed to C-O-C stretching,[31] vary in shape and intensity with the addition of different salts. These changes possibly indicate that there is an interaction between C-O-C groups and Zn-ions, but it can also be a contribution of the Zn-salt in itself, in particular for $Zn(OTf)_2$ (see FTIR spectra of salts in Supporting information, Figure S2). The band at 3200–3500 cm^{-1} attributed to hydroxyl stretching vibration and the band at 1640 cm^{-1} attributed to H-O-H deformation vibration,[32–33] also indicate that HEC-films contain traces of water, similar with all salts. On the contrary, PEO-films seem to contain less water, and the amount depends on the added Zn-salt.

2.2 | Influence of Zn-salt on ionic conductivity of HEC films

The conductivity of HEC films, presented in Figure 3A, shows very low values, from 10^{-11} S cm^{-1} at 0°C to 10^{-6} S cm^{-1} at 110°C. This is far below the threshold of 0.1 mS cm^{-1} set for practical battery applications. In fact, most of HEC/Zn-salt films show a lower conductivity than the pure HEC film at low temperature and slightly higher conductivity at the region of high temperature. The conductivity, σ, is a sum of several contributions, not only from Zn^{2+} but also from other ions present, such as the anion of the salt and also H^+ if water is present. HEC and PEO have a negligible electronic conductivity, but the strong

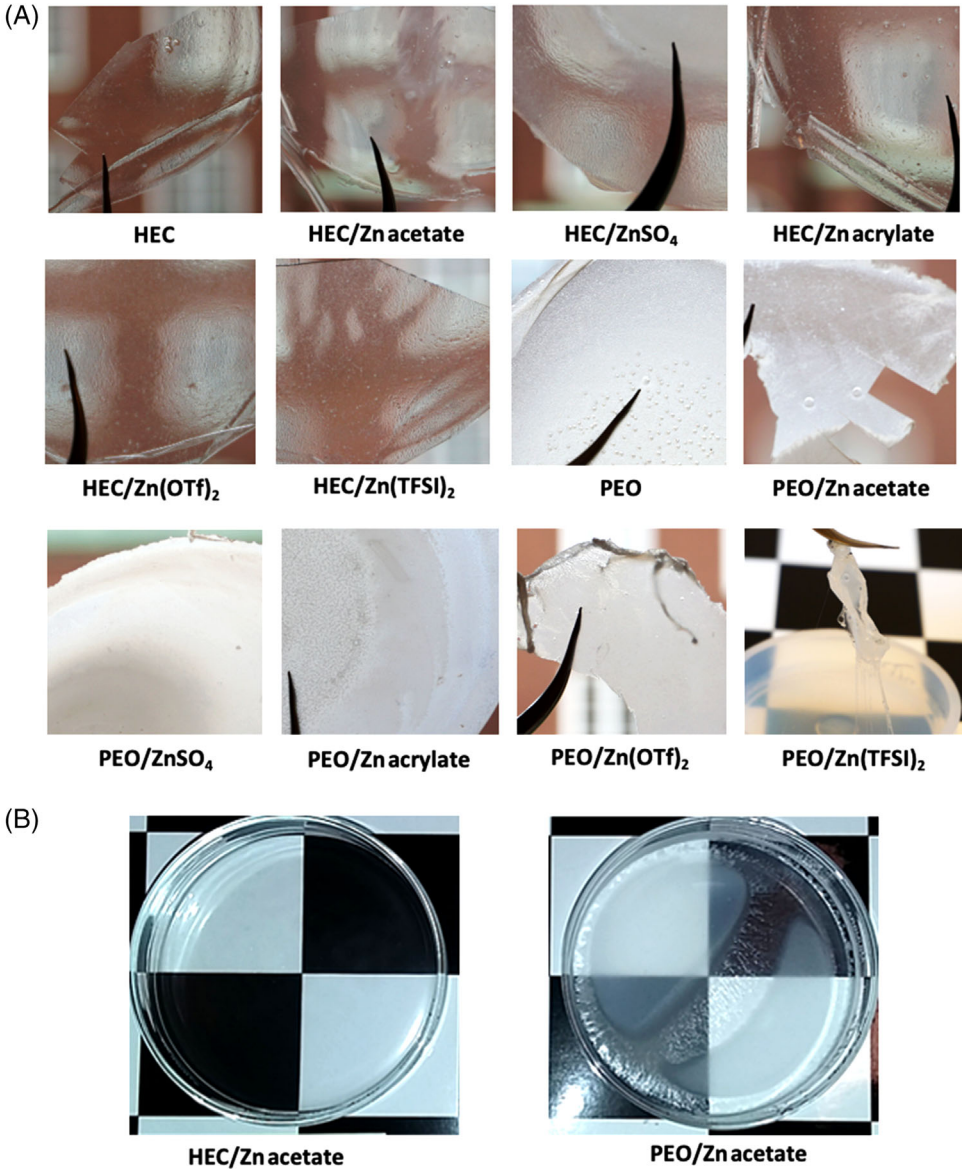

FIGURE 1 Preparation of solid electrolyte films. A, Images of thin films prepared with a ratio of ether oxygen to zinc ion (EO:Zn^{2+}) of 20:1, and dried at 50°C. B, Images of HEC/Zn acetate and PEO/Zn acetate thin films dried at room temperature

hygroscopicity of HEC should be considered for proton conductivity.[34] Proton conductivity in HEC films could explain the higher conductivity of pure HEC, since the preparation process of polymer electrolytes can change the water content and thus influence the overall conductivity.

Usually, the ionic conductivity of a polymer electrolyte is strongly dependent on its melting point and glass transition temperature, which can be determined by differential scanning calorimetry (DSC). The DSC traces of HEC, shown in Figure 3B, indicate that HEC is an amorphous polymer, which is in line with the WAXS results, and its glass transition temperature is around 100°C. Addition of Zn-salts like $ZnSO_4$ or Zn acetate shows little influence on the thermal behavior of HEC films and only slightly shifts the glass transition temperature (T_g). Addition of $Zn(TFSI)_2$, on the other hand, brings an obvious decrease of T_g down to 50°C, underlining the strong plasticizing effect of the TFSI anion. In general, conductivity is expected to be significantly enhanced when the temperature is above T_g since segmental motion of polymer chains is facilitated. However, no observable change in behavior is detected in the conductivity below and above 50°C for HEC/$Zn(TFSI)_2$. Moreover, the addition of $Zn(TFSI)_2$ gives the lowest conductivity among all HEC/Zn-salt films at low temperature, which is unexpected in view of the DSC results. However, the transport of Zn-ions in

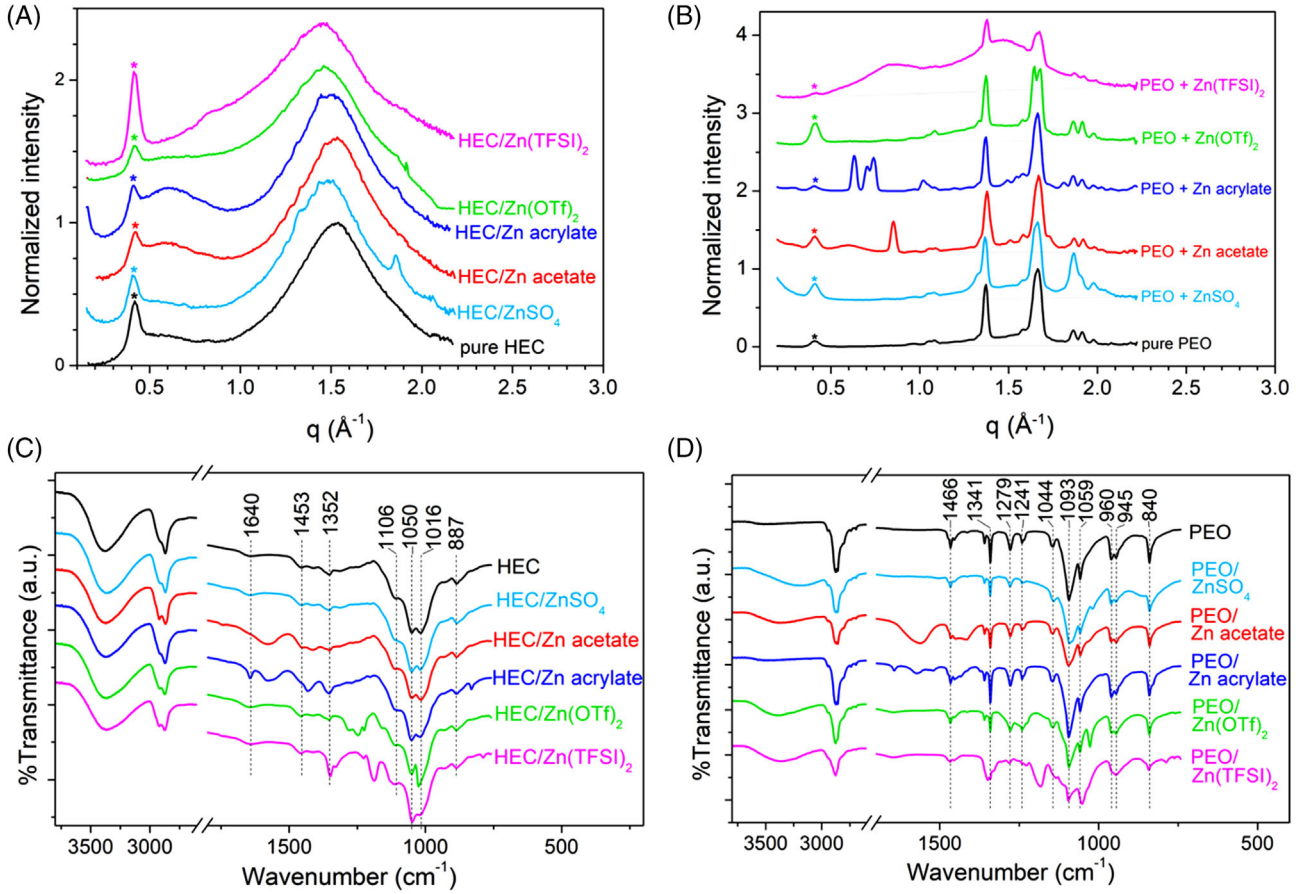

FIGURE 2 Structure of solid electrolyte films. A-B, WAXS profiles of HEC thin films and PEO thin films. Peaks labeled * are related to Kapton windows used in the sample cells and are not part of the sample. C-D, Fourier-transform infrared spectra (FTIR) of PEO and HEC films. Main peaks of the neat polymer are indicated by dashed lines. 2600–1800 cm^{-1} region has been left out since no peak appears there

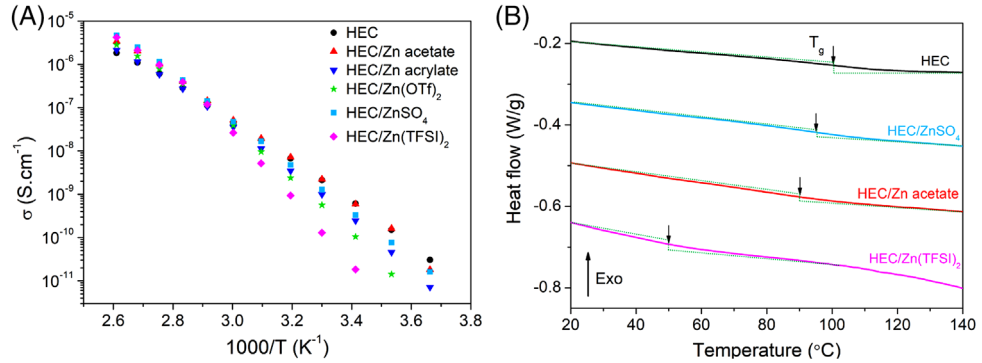

FIGURE 3 Properties of HEC films with different Zn-salts. A, Ionic conductivity as a function of temperature for HEC films containing various Zn-salts with a ratio of EO:Zn^{2+} of 20:1. B, Differential scanning calorimetry (DSC) traces of HEC films. Approximate positions of glass transitions are indicated by thin arrows

polymer matrix is also strongly dependent on the molecular structure apart from the T_g of polymer.[35] The molecular of HEC only consists of short sidechains as complexation sites, showing a much lower salt-dissociation capability which will lead to the low ionic conductivity.

2.3 | Influence of water on ionic conductivity of HEC films

To determine the influence of water content on the conductivity, HEC, HEC/Zn acetate, and HEC/Zn(TFSI)$_2$ films

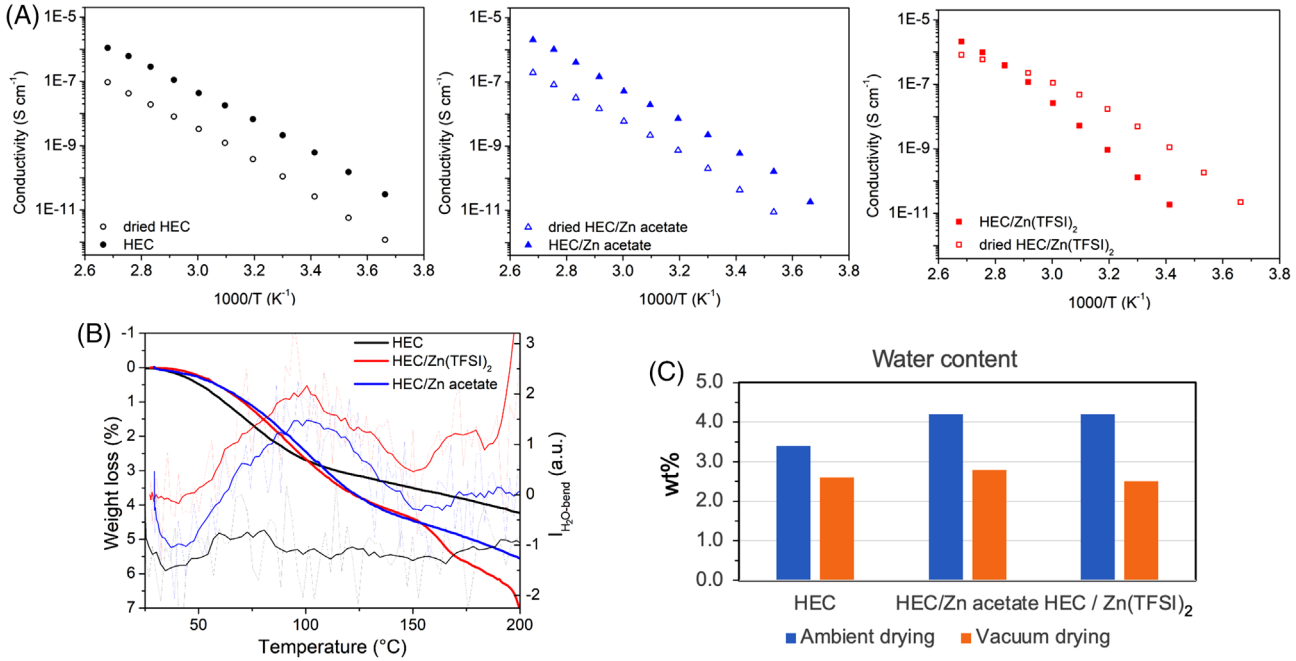

FIGURE 4 Influence of water content on conductivity of HEC films. A, Conductivities of HEC, HEC/Zn acetate and HEC/Zn(TFSI)$_2$ before and after drying under vacuum at room temperature for 24 h. B, Thermogravimetric analysis (TGA) of HEC films before drying. Thick curves show the mass loss as a function of temperature, and thin curves are a smoothing of the light dashed lines, which are IR intensity of H_2O-bend of emission gases. C, Estimated water content in three HEC films before and after drying, calculated from mass loss at 140°C in TGA

were dried under vacuum for 12 h at room temperature to remove water. Conductivity measurement was then performed again on these partially dried samples, Figure 4A. A quantitative analysis of water content in the films was conducted by thermogravimetric analysis (TGA) (Figure 4B,C). The first step of weight loss in the TGA curves corresponds to the loss of water, as shown by the FTIR analysis of emitted gases (Figure 4B) and the water content of the HEC films is estimated by the weight loss at 140°C (Figure S3).

It is observed that the water content is slightly higher in the HEC films containing Zn-salt, suggesting that this change of water content is directly related to the conductivities shown in Figure 4A. However, the conductivity of the pure HEC film and the HEC/Zn acetate film decreases one order of magnitude after having been partially dried. On the contrary, removing water from HEC/Zn(TFSI)$_2$ enhances the ionic conductivity at low temperature but slightly decreases it at high temperature. These results suggest that the role of water on the ionic conductivity of HEC films is complex. On one hand, presence of water could be helpful to dissociate the zinc salt, and water can also act as a plasticizer to reduce the glass transition temperature of polymer matrix, enhancing the dissociation capability for Zn salt. On the other hand, water could compete with the polymer chains to associate Zn^{2+}, decreasing the mobility of ions. Furthermore, the conduction of protons also contributes to the overall conductivity of the films. More investigations would be needed for a better understanding of the contribution of water to the conductivity of polymer electrolytes.

2.4 | Influence of Zn-salt on ionic conductivity for PEO films

Unlike the HEC films, the conductivities of the PEO films show a strong dependence on the type of Zn-salt, Figure 5A. PEO films containing Zn acetate, Zn acrylate or $ZnSO_4$ show an enhanced conductivity compared to pure PEO, but their conductivities fall rapidly below 70°C due to the crystallinity of the polymer. On the contrary, PEO films containing Zn(OTf)$_2$ or Zn(TFSI)$_2$ have a much higher conductivity even at low temperature (10^{-5} S cm^{-1} at 20°C). The different behavior of the conductivity is mainly due to the plasticizing ability of the anion. The DSC traces in Figure 5B show that $TFSI^-$ has the strongest plasticizing effect among all anions, since no melting peak is found in the trace from the PEO/Zn(TFSI)$_2$ film. For the other anions, a smaller area of the melting peak and a lower melting temperature also shows on a plasticizing effect. The peak area and the relative crystallinity with respect to pure PEO have been calculated and shown in Figure 5C. It is observed that Zn acetate is a weaker plasticizer than Zn acrylate, even if the PEO film with Zn acetate shows a higher conductivity than the

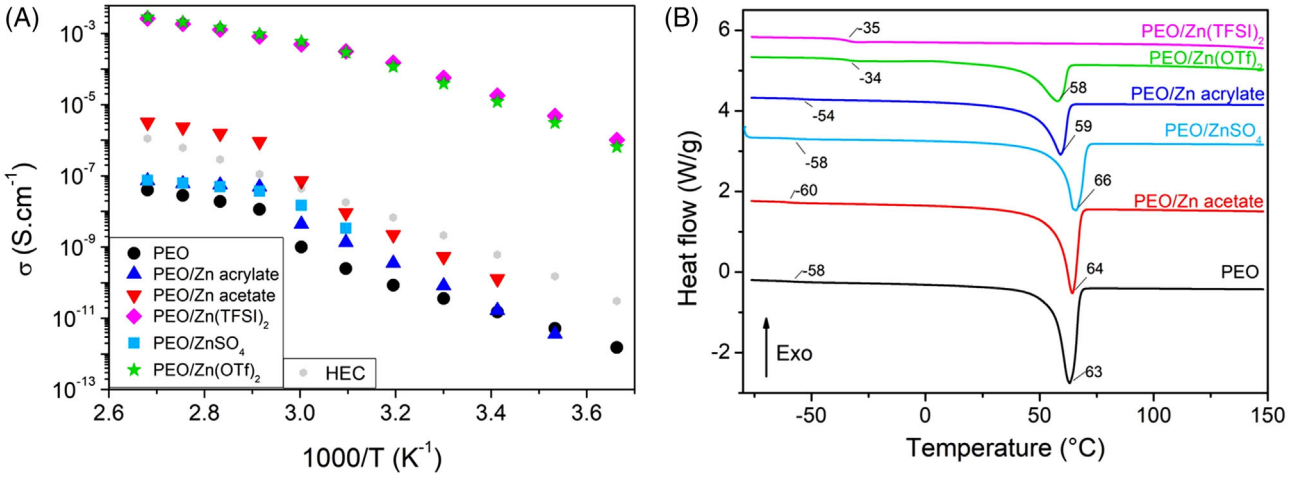

(C)

	PEO	PEO/Zn acetate	$PEO/ZnSO_4$	PEO/Zn acrylate	$PEO/Zn(OTf)_2$	$PEO/Zn(TFSI)_2$
Peak area	22.22	19.89	16.91	13.77	11.98	0
Relative crystallinity	100%	89.5%	76.1%	62.0%	53.9%	0%

FIGURE 5 Properties of PEO films with different Zn-salts. A, Ionic conductivity as a function of temperature of PEO films containing various Zn-salts with a ratio of $EO:Zn^{2+}$ of 20:1. Grey dots represent conductivity of pure HEC as a comparison. B, DSC traces of PEO/Zn-salt films. Glass transition and melting temperatures are indicated for each curve. C, Areas of melting peaks and calculated crystallinity of the PEO films

one with Zn acrylate. Thus, the plasticizing effect is not the only factor to influence the conductivity of PEO solid electrolytes.

As previously discussed for SPE films, water could also play a significant role on the conductivity.[36] In addition, the lattice energy and concentration of Zn-salts are two other important parameters to consider, since they determine the number of dissociated ions in the polymer matrix. The conductivity depends on the concentration of free ions rather than on the total concentration of salt in the polymer matrix. In some cases, increasing the concentration of salt can lead to ion aggregation and reduced chain mobility, thus decreasing conductivity.

2.5 | Influence of salt concentration on ionic conductivity of HEC films

To investigate the influence of salt concentration on the conductivity, HEC/Zn acetate films were prepared with various ratios of $EO:Zn^{2+}$, n = 4:1, 10:1, 20:1, 50:1 and 100:1. The conductivity as a function of temperature of these films is shown in Figure 6A. For a given temperature, the conductivity first increases with increasing concentration of Zn-salt (decreasing n), then decreases, and finally increases again at high concentration. The final increase of ionic conductivity at high salt concentration of 4:1 is resulted from reduced crystallinity of polymer and slight increase of free ions.[26,37] The salt concentration giving the highest conductivity is dependent on the temperature range, going from 4:1 at low temperature to 50:1 at high temperature. However, previous studies on PEO/salt system show that the dependence of conductivity on salt concentration is complex.[6] Therefore, further investigations on other concentrations would be needed to determine if there is a real evolution of conductivity as a function of concentration, rather than fluctuations among samples. Moreover, the FTIR spectra in Figure 6B suggest that the amount of water in HEC films varies between the samples. This phenomenon could also contribute to the fluctuations of conductivity.

In this work we focus on the preparation and structure characterization of HEC based polymer electrolytes for solid state Zn batteries. Our results also show insightful perspective for future design of polymer electrolyte. (1) Both the polymer matrix and salt play a significant role on the mechanical property of polymer electrolyte, which is the premier factor to the formation of thin membrane. (2) The ionic conductivity of polymer electrolytes is highly dependent on the glass transition temperature and salt-dissociation capability of polymer matrix. (3) Selection of salt is critical to the glass transition temperature of polymer electrolyte and this plasticizing effect is also related to the repeated coordination/dissociation of ions with polymer complexation sites, promising the transport of ions in polymer matrix.

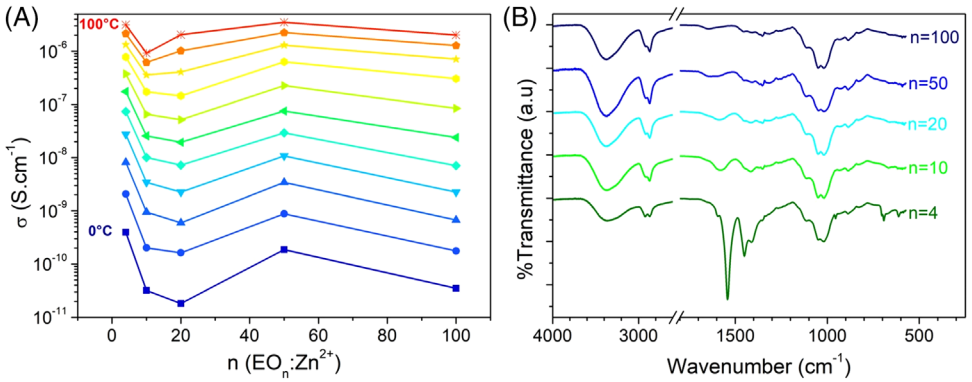

FIGURE 6 Influence of the concentration of Zn acetate in HEC films. A, Isotherms of conductivity as a function of composition ($n = 4$, 10, 20, 50, and 100, n is the ratio of ether oxygens to Zn ions). B, FTIR spectra of HEC films. The 2600–1800 cm^{-1} region has been left out since no peaks appear there

3 | CONCLUSION

In this work, solid polymer electrolytes have been prepared from HEC and PEO polymers with various zinc salts. HEC shows a good film-forming ability and a satisfactory solubility of zinc salts. However, the HEC-based films show a low conductivity which is virtually independent of type of zinc salt. On the contrary, the properties of PEO-based films strongly depend on the type of zinc salt, and in particular on the plasticizing ability of this salt. With zinc salts that are weak plasticizers, the conductivity of PEO films shows a strong temperature-dependence and overall remains low due to the high crystallinity of the polymer. When good plasticizers were added, such as $Zn(TFSI)_2$, PEO films show a high conductivity but are difficult to process due to their poor mechanical properties, being very soft and sticky. In both HEC- and PEO-based films, the role of water on the conductivity is complex and should be further investigated. Furthermore, the dependence of conductivity of HEC-based electrolytes on concentration of zinc acetate has also been investigated and future work should be continued to clarify this relation.

4 | EXPERIMENTAL SECTION

4.1 | Materials

Zinc acetate dihydrate ($Zn(CH_3COO)_2{\cdot}2H_2O$), zinc acrylate ($Zn(CH_2CHCO_2)_2$), zinc bis(trifluoromethansulfonyl)imide ($Zn(TFSI)_2$), zinc sulfate heptahydrate ($ZnSO_4{\cdot}7H_2O$) and zinc trifluoromethanesulfonate ($Zn(OTf)_2$) were purchased from Sigma-Aldrich Inc. with ≥ 98% purity (except from $Zn(TFSI)_2$ with 95% purity). Hydroxyethylcellulose (HEC, Natrosol 250G) powder with an average molecular weight of 300,000 Da and poly(ethyleneoxide) (PEO, Polyox WSR N60K) powder with an average molecular weight of 2,000,000 Da were chosen to prepare the thin films. All materials were used as received without any further purification.

4.2 | Preparation of solid polymer electrolyte

For the PEO-based films, the mass ratio of polymer and salt was determined by setting a ratio of ether oxygen:zinc cation ($EO:Zn^{2+}$) to 20:1. It means that there are 20 monomers of PEO per Zn ion, with $M_{PEO\ monomer} = 44.05$ g mol^{-1}. For the HEC-based films, the same ratio of $EO:Zn^{2+}$ (20:1) was chosen, except for the investigation of the influence of salt concentration where it varies from 100:1 to 4:1. It was assumed that an average of 5 ethylene oxide units are attached to one cellulose monomer, thus the ratio of HEC monomer:Zn^{2+} corresponding to a ratio of $EO:Zn^{2+}$ of 20:1 was determined as 4:1. The molecular weight of a single HEC monomer was estimated as $M_{cellulose\ monomer} + 5 \times M_{ethylene\ oxide} = 544.53$ g mol^{-1}. The calculated amount of polymer and salt were dissolved in water at room temperature under stirring to obtain a homogeneous solution. The solution was then casted onto a glass Petri dish and heated to 50μC (unless otherwise specified) overnight to evaporate water to obtain a thin film of 100–300 μm thickness. The film was then left 2 days under ambient atmosphere, protected from dust, until it reached equilibrium with ambient moisture.

4.3 | Ionic conductivity measurements

Electrochemical impedance spectroscopy was performed with a Novocontrol Concept 40 broadband dielectric

spectrometer. A thin film disk with a diameter of 2.5 cm was placed between two stainless steel blocking electrodes under pressure. Impedance measurements were conducted in a frequency range of 10^{-1} –10^{7} Hz at different temperatures, starting from the lowest. The bulk resistance R_b was obtained from Nyquist plots (Z' vs. −Z'') as explained in Figure S4 in Supporting information.[38] For PEO samples, conductivity below melting temperature was calculated taking the initial thickness, and conductivity above melting temperature was calculated from the final thickness.

4.4 | Structure characterization

FT-IR spectra were obtained with a Bruker IFS 66v FTIR spectrometer equipped with Globar Source, KBr MIR beam splitter, DTGS MIR detector and Imaging Golden Gate Diamond ATR accessory. Spectra were recorded under vacuum by 10 scans with a resolution of 2 cm^{-1} in the range 400–4000 cm^{-1}. X-ray scattering patterns were collected using a Mat: Nordic X-Ray scattering instrument equipped with a high brilliance Rigaku 003 X-Ray microfocus Cu-radiation source (λ = 1.54 Å) and a Pilatus 300 K detector. The samples were enclosed in a sandwich cell with Kapton (polyimide) windows and measured at room temperature with an exposure time of 200 s and a sample-to-detector distance of 134 mm. Thermal characterization of the samples was performed using a TA Instruments DSC250 Discovery. A small amount of sample (5–10 mg) was sealed in a hermetic aluminum pan and then subjected to a heat-cool-heat cycle from −80μC to 150μC for PEO samples and from 0μC to 200μC for HEC samples, with a heating and cooling rate of 10μC min^{-1}. To evaluate water content in samples, thermogravimetric analyses were performed using a Netzsch TG 209 F1, coupled with a Bruker Vector 22 FT-IR spectrometer. A small amount of sample (∼10 mg) was placed in an aluminum crucible and heated from 25μC to 400μC with a rate of 10μC min^{-1} under a nitrogen purge gas flow of 100 ml min^{-1}. Emission gases were analyzed by FTIR to monitor the release of water.

ACKNOWLEDGMENTS

The Knut and Alice Wallenberg Foundation is acknowledged, through the Wallenberg Wood Science Center (WWSC), and the Excellence Initiative Nano at Chalmers University of Technology are acknowledged for financial support. The Ecole Normale Supérieure (Paris) is gratefully acknowledged for financial support for internship of A.B.

CONFLICT OF INTEREST

The authors declare no conflict of interest.

DATA AVAILABILITY STATEMENT

The datasets in this study are available from the corresponding author on reasonable request.

REFERENCES

1. S. Chu, Y. Cui, N. Liu, *Nat. Mater.* **2016**, *16*, 16.
2. J. M. Tarascon, M. Armand, *Nature* **2001**, *414*, 359.
3. C. P. Grey, D. S. Hall, *Nat. Commun.* **2020**, *11*, 6279.
4. S. S. Shinde, J. Y. Jung, N. K. Wagh, C. H. Lee, D.-H. Kim, S.-H. Kim, S. U. Lee, J.-H. Lee, *Nat. Energy* **2021**, *6*, 592.
5. L. Ma, M. A. Schroeder, O. Borodin, T. P. Pollard, M. S. Ding, C. Wang, K. Xu, *Nat. Energy* **2020**, *5*, 743.
6. J. Wang, Y. Yang, Y. Zhang, Y. Li, R. Sun, Z. Wang, H. Wang, *Energy Storage Mater.* **2021**, *35*, 19.
7. C. Han, W. Li, H. K. Liu, S. Dou, J. Wang, *Nano Energy* **2020**, *74*, 104880.
8. K. Wu, J. Huang, J. Yi, X. Liu, Y. Liu, Y. Wang, J. Zhang, Y. Xia, *Adv. Energy Mater.* **2020**, *10*, 1903977.
9. J. Song, K. Xu, N. Liu, D. Reed, X. Li, *Mater. Today* **2021**, *45*, 191.
10. Q. Liu, R. Liu, C. He, C. Xia, W. Guo, Z.-L. Xu, B. Y. Xia, *eScience* **2022**, *2*, 453.
11. C. Xia, Y. Zhou, C. He, A. I. Douka, W. Guo, K. Qi, B. Y. Xia, *Small Science* **2021**, *1*, 2100010.
12. Q. Zhao, S. Stalin, C.-Z. Zhao, L. A. Archer, *Nat. Rev. Mater.* **2020**, *5*, 229.
13. J. Lopez, D. G. Mackanic, Y. Cui, Z. Bao, *Nat. Rev. Mater.* **2019**, *4*, 312.
14. D. Zhou, D. Shanmukaraj, A. Tkacheva, M. Armand, G. Wang, *Chem* **2019**, *5*, 2326.
15. J. Wu, Z. Rao, Z. Cheng, L. Yuan, Z. Li, Y. Huang, *Adv. Energy Mater.* **2019**, *9*, 1902767.
16. R. C. Agrawal, G. P. Pandey, *J. Phys. D Appl. Phys.* **2008**, *41*, 223001.
17. Z. Gadjourova, Y. G. Andreev, D. P. Tunstall, P. G. Bruce, *Nature* **2001**, *412*, 520.
18. Q. Zhao, X. T. Liu, S. Stalin, K. Khan, L. A. Archer, *Nat. Energy* **2019**, *4*, 365.
19. C. Wang, T. Wang, L. Wang, Z. Hu, Z. Cui, J. Li, S. Dong, X. Zhou, G. Cui, *Adv. Sci.* **2019**, *6*, 1901036.
20. C. Hänsel, E. Lizundia, D. Kundu, *ACS Appl. Energy Mater.* **2019**, *2*, 5686.
21. Y.-Y. Li, B. Wang, M.-G. Ma, B. Wang, *Int. J. Polym. Sci.* **2018**, *2018*, 1.
22. S. Wang, L. Zhang, Q. Zeng, X. Liu, W.-Y. Lai, L. Zhang, *ACS Sustain. Chem. Eng.* **2020**, *8*, 3200.
23. I. Dueramae, M. Okhawilai, P. Kasemsiri, H. Uyama, R. Kita, *Sci. Rep.* **2020**, *10*, 12587.
24. L. Cao, D. Li, T. Pollard, T. Deng, B. Zhang, C. Yang, L. Chen, J. Vatamanu, E. Hu, M. J. Hourwitz, L. Ma, M. Ding, Q. Li, S. Hou, K. Gaskell, J. T. Fourkas, X.-Q. Yang, K. Xu, O. Borodin, C. Wang, *Nat. Nanotechnol.* **2021**, *16*, 902.
25. H. Luo, B. Liu, Z. Yang, Y. Wan, C. Zhong, *Electrochem. Energy Rev.* **2022**, *5*, 187.
26. W. Wieczorek, D. Raducha, A. Zalewska, J. R. Stevens, *J. Phys. Chem. B* **1998**, *102*, 8725.
27. C. P. Rhodes, R. Frech, *Solid State Ionics* **1999**, *121*, 91.
28. S. Zhang, N. Yu, S. Zeng, S. Zhou, M. Chen, J. Di, Q. Li, *J. Mater. Chem. A* **2018**, *6*, 12237.

29. A. M. Hyde, S. L. Zultanski, J. H. Waldman, Y.-L. Zhong, M. Shevlin, F. Peng, *Org. Process Res. Dev.* **2017**, *21*, 1355.
30. X. Lu, E. J. Hansen, G. He, J. Liu, *Small* **2022**, *18*, 2200550.
31. P. Dhatarwal, R. J. Sengwa, *Macromol. Res.* **2019**, *27*, 1009.
32. S. Chaouf, S. El Barkany, I. Jilal, Y. El Ouardi, M. Abou-salama, M. Loutou, A. El-Houssaine, H. El-Ouarghi, A. El Idrissi, H. Amhamdi, *J. Water Process Eng.* **2019**, *31*, 100807.
33. J. Kozlowska, N. Stachowiak, A. Sionkowska, *Polymers* **2018**, *10*, 456.
34. L. V. S. Lopes, G. O. Machado, A. Pawlicka, J. P. Donoso, *Electrochim. Acta* **2005**, *50*, 3978.
35. Y. Zhang, Z. Chen, H. Qiu, W. Yang, Z. Zhao, J. Zhao, G. Cui, *NPG Asia Mater.* **2020**, *12*, 4.
36. D. Mankovsky, D. Lepage, M. Lachal, L. Caradant, D. Aymé-Perrot, M. Dollé, *Chem. Commun.* **2020**, *56*, 10167.
37. J. Gurusiddappa, W. Madhuri, R. Padma Suvarna, K. Priya Dasan, *Mater* **2016**, *3*, 1451.
38. S. B. Aziz, T. J. Woo, M. F. Z. Kadir, H. M. Ahmed, *J. Sci. Adv. Mater. Dev.* **2018**, *3*, 1.

SUPPORTING INFORMATION

Additional supporting information can be found online in the Supporting Information section at the end of this article.

How to cite this article: A. Brige, M. Olsson, S. Xiong, A. Matic, *Nano Select*. **2023**, *4,* 102. https://doi.org/10.1002/nano.202200221